Journal of Sensor Science and Technology
Vol. 27, No. 4 (2018) pp. 216-220
http://dx.doi.org/10.5369/JSST.2018.27.4.216
pISSN 1225-5475/eISSN 2093-7563

Visual Sensing of the Light Spot of a Laser Pointer for Robotic Applications

Sung-Ho Park[1], Dong Uk Kim[1], and Yongtae Do[2+]

Abstract

In this paper, we present visual sensing techniques that can be used to teach a robot using a laser pointer. The light spot of an off-the-shelf laser pointer is detected and its movement is tracked on consecutive images of a camera. The three-dimensional position of the spot is calculated using stereo cameras. The light spot on the image is detected based on its color, brightness, and shape. The detection results in a binary image, and morphological processing steps are performed on the image to refine the detection. The movement of the laser spot is measured using two methods. The first is a simple method of specifying the region of interest (ROI) centered at the current location of the light spot and finding the spot within the ROI on the next image. It is assumed that the movement of the spot is not large on two consecutive images. The second method is using a Kalman filter, which has been widely employed in trajectory estimation problems. In our simulation study of various cases, Kalman filtering shows better results mostly. However, there is a problem of fitting the system model of the filter to the pattern of the spot movement.

Keywords: Visual sensing, Laser pointer, Trajectory estimation, Kalman filter, Robot vision

1. INTRODUCTION

Robotics has been rapidly growing in recent years, and robots of various forms are employed in diverse applications unlike traditional industrial robots that have been fixed on the factory floor for limited tasks. A smart robot should be equipped with a high-level sensing technology so that it can cope with dynamic surrounding situations properly [1]. Vision is the highest level sensor among various sensing capabilities in robotics. There have been many studies on robot vision for a long time, and the object recognition technique using artificial intelligence including deep learning has been greatly developed [2]. However, it is still difficult for a robot to recognize the target of a task among various objects particularly in scattered surroundings. Even when an autonomous robot with vision sensing capability is used to provide services to people, an efficient interface between humans and the robot is still important.

Laser pointers are widely used in projector-based presentations to draw audience's attention to a specific part of the presentation. As a laser pointer has significant potential for the man–machine interface, there have been attempts to use laser pointers in robotics as we did in smart presentation [3]. For example, a laser pointer is utilized to guide a home service robot by its user [4]. A robot cell calibration method is proposed based on simple laser sensing methods [5]. A laser pointer is used to guide an underwater mobile robot for reactor vessel inspection [6]. The use of laser pointers can be much simpler and more straightforward in the man–robot interface than methods employed in many previous studies such as understanding human language [7] and interpreting hand gestures [8].

In this paper, we present vision sensing techniques to use a laser pointer in robotic applications. The system can be constructed using a laser pointer, a color camera, and a PC. The sensing algorithm consists of image processing of laser spot detection, tracking, and three-dimensional (3D) position computation. First, the spot of a laser pointer is detected by multistep image processing as proposed in Section 2.1. Second, two methods are discussed in Section 2.2 to track the laser spot in consequent images. The 3D position of the laser spot can then be calculated by stereoscopy as shown in Section 2.3.

[1]Dept. of Electronic Engineering, Graduate School, Daegu University, 201 Daegudae-ro, Gyeongsan-si, Gyeongsangbuk-do, 38453, Korea
[2]Division of Electronic Control Engineering, School of Electronic and Electrical Engineering, Daegu Unversity, 201 Daegudae-ro, Gyeongsan-si, Gyeongsangbuk-do, 38453, Korea
[+]Corresponding author: ytdo@daegu.ac.kr
(Received: Jul. 15, 2018, Revised: Jul. 25, 2018, Accepted: Jul. 27, 2018)

2. VISUAL SENSING OF THE LASER SPOT

2.1 Detection

The first procedure in the proposed system is the detection of the light spot of a laser pointer on a camera image. We detect the spot by a multistep algorithm presented in Fig. 1. First, when laser light is assumed red, a monochrome image is obtained by selecting only the R (red) channel of the R, G (green), and B (blue) colors of the camera. Then, bright pixels are detected by comparing the pixel values with a threshold. By these two processing steps, bright pixels on the R image are selected, which results in a binary image. In the third step, small holes inside foreground blobs are removed by morphological closing, dilation then erosion, which is written in operator form as

$$I \bullet S = (I \oplus S) \ominus S \tag{1}$$

where I is the binary image processed, S is the structuring element for the morphological pixel operation, • means closing, $\ominus$ means erosion, and $\oplus$ is dilation. The next processing step is to check the size and shape of the blobs. Since the laser spot is small and round, the window shown in Fig. 2 is used in the check. If a blob on I is the laser light spot, the outline pixels in the window are 0, and the pixels in the center portion are 1. This can be verified by the equation below

$$\sum_{(i,j) \in W} I(i,j) - \sum_{(i,j) \in O} I(i,j) \le \lambda \tag{2}$$

where W is the window, O is the center portion of the window, (i,j) are the image coordinates, and λ is a threshold. The threshold is ideally zero, but may be larger due to some noise and error. Eq. (2) means that the sum of all pixel values in the window should be approximately equal to the sum of the pixel values in the central portion. The shape of the center portion should be a circle, but we define it as a square for the convenience of calculation.

The light spot can be extracted through the steps above, but noisy spots smaller than the light spot can be also detected. The morphological erosion operations are performed several times to eliminate small noisy spots. Then, the size of the light spot can be restored to its original size by performing the dilation operation several times. The position of the light spot detected can be calculated by

$$x = M_{10}/M_{00}\,,\ y = M_{01}/M_{00} \tag{3}$$

where M is the moment of the binary image defined as

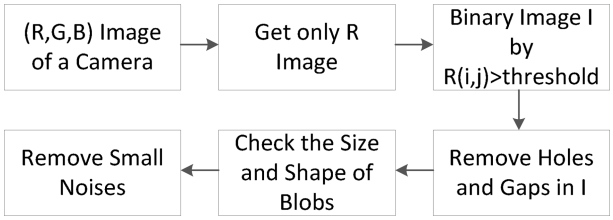

Fig. 1. Image processing to detect the light spot of a laser pointer.

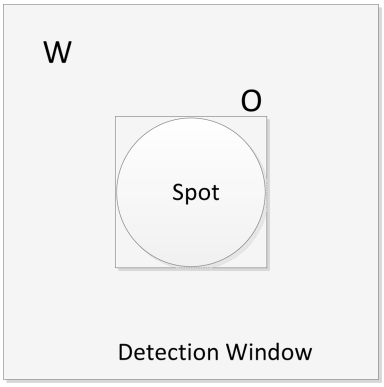

Fig. 2. Window to check the size and shape of a foreground blob detected in the binary image.

$$M_{pq} = \sum_{(i,j) \in I} i^p j^q I(i,j) \tag{4}$$

2.2 Tracking

When the light spot of a laser pointer moves, the movement is tracked in consecutive images. In this study, we predict the position where the laser spot can be detected and estimate the actual position from the measured position, so that it is possible to perform robust and efficient tracking even under noisy conditions.

Two methods are used for the tracking. The first method, called as Method I, is simply to use the position of the currently detected light spot, (x_t, y_t), to find the laser spot position in the next image, (x_{t+1}, y_{t+1}). That is, the region of interest (ROI) in an image having a predetermined size is set around the current laser spot position, and the spot is detected within the ROI of the next image. This method assumes that the movement speed of the laser spot between two consecutive images is sufficiently low.

The second method is Kalman filtering (Method II). The state variable P in the filter is defined as the position coordinates (x, y) and their velocities (v_x, v_y) of the laser spot as

$$P = [x \quad v_x \quad y \quad v_y]^T \tag{5}$$

Now, the filter model is

$$P_{t+1} = AP_t + \omega_t\,,\ Z_t = HP_t + n_t \tag{6}$$

where w is the system noise, n is the measurement noise, and the system matrices are as the below

$$A=\begin{bmatrix}1 & \Delta t & 0 & 0\\ 0 & 1 & 0 & 0\\ 0 & 0 & 1 & \Delta t\\ 0 & 0 & 0 & 1\end{bmatrix},\ H=\begin{bmatrix}1 & 0 & 0 & 0\\ 0 & 0 & 1 & 0\end{bmatrix}$$

Then, the prediction, $\hat{P}_t^-$, and the estimation, $\hat{P}_t$, of the state P are obtained by the standard Kalman filter algorithm [9]. The ROI in which the laser spot is searched in the next image frame is set around the predicted position $\hat{P}_t^-$.

2.3 Calibration for 3D Sensing

When a robot needs the 3D position of the laser spot, which is pointed on a target object, stereo cameras are required. The relation between the 3D space and each camera plane of the stereo can be determined by calibration. We use the pinhole camera model shown in Fig. 3 for calibration [10]. A 3D world point at (X,Y,Z) can be related to its image point at (x,y) by

$$(sx\ \ sy\ \ s)^T = C(X\ \ Y\ \ Z\ \ 1)^T \tag{7}$$

where s is a scale factor and C is the camera matrix. To determine the elements of the matrix, Eq. (7) is written as

$$x=\frac{c_{11}X+c_{12}Y+c_{13}Z+c_{14}}{c_{31}X+x_{32}Y+c_{33}Z+c_{34}} \tag{8.1}$$

$$y=\frac{c_{21}X+c_{22}Y+c_{23}Z+c_{24}}{c_{31}X+c_{32}Y+c_{33}Z+c_{34}} \tag{8.2}$$

where $c_{ij},\ i=1,2,3,\ j=1,2,..,4,$ are the elements of C. Then, the matrix elements are found by solving

$$\begin{pmatrix}X\ Y\ Z\ 1\ 0\ 0\ 0\ 0\ -Xx\ -Yx\ -Zx\\ 0\ 0\ 0\ 0\ X\ Y\ Z\ 1\ -Xy\ -Yy\ -Zy\end{pmatrix}\begin{pmatrix}c_{11}\\ \cdots\\ c_{33}\end{pmatrix}=\begin{pmatrix}x\\ y\end{pmatrix} \tag{9}$$

After calibrating another camera by the same procedure described above, we can compute the 3D position of the spot from two corresponding images of the spot. Although image correspondence is a major difficulty in stereo vision, it is straightforward in this paper because the corresponding laser spots can be detected by the method of Section 2.1.

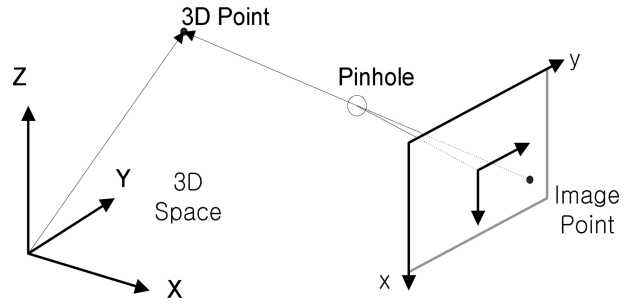

Fig. 3. Pinhole camera model for calibration between the 3D space and the 2D image plane of a camera.

3. RESULTS

Experiments were conducted to check the system presented in this paper. In order to test the proposed method of detecting the light spot in an image, we measured the light spot of a red laser pointer on a real camera image. Fig. 4 shows an example of the results obtained using the proposed method. Fig. 4(b) shows the R monochrome image of Fig. 4(a). The scene was arranged to contain several red components, such as a marker, a board eraser, and characters in addition to shiny white background to reflect bright lighting. This arrangement made the detection of the red laser spot difficult. Fig. 4(c) shows pixels with brightness of 250 or greater. As a result of size and shape filtering using the detection window and the morphological operations, we could get an image shown in Fig. 4(d), which is the negative image in order to show the result more clearly. In this figure, the laser light spot is well detected in spite of cluttered surroundings.

The laser light spot tracking was performed by applying the two methods discussed in Section 2.2. We used the data generated artificially in order to analyze the results for various cases. Table 1 shows the characteristics of the data used in this simulation study. <DATA 1> is the case where the data are measured at intervals of 0.03 second for the laser spot moving at a constant speed. The measurement error was assumed to follow a normal distribution with zero mean and a standard deviation of 1 pixel. <DATA 2> is the spot position trajectory data generated assuming a constant acceleration. <DATA 3> was simulated for a mixed movement pattern where the spot was assumed moving at a constant acceleration first and at a constant velocity later. <DATA 4> is a complicated angular movement of a constant acceleration first, constant velocity second, and constant deceleration third.

Table 2 shows the results of the laser light spot tracking. The two methods tested successfully tracked the light spot, but the Kalman filter showed better performance mostly except the case of <DATA 4>. The reason may be that the movement in the data was made in the angular space, while the Kalman filter estimated the spot position in the Cartesian space. Therefore, the system model of the filter did not fit well to the data. The quite large error could be reduced significantly by adjusting the process and measurement noise covariance matrices. Fig. 5 shows the tracking

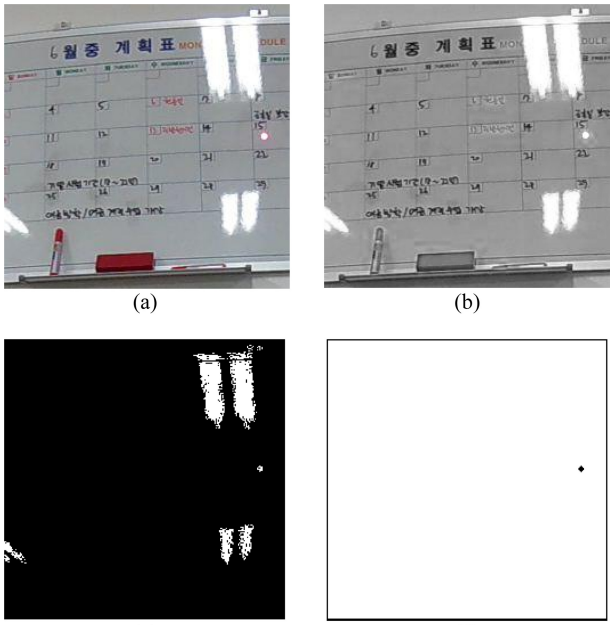

(a) (b) (c) (d)

Fig. 4. Laser spot detection. (a) Input color image, (b) R channel monochrome image, (c) Detected bright pixels, and (d) Detected laser spot after size and shape filtering in addition to morphological operations.

Table 1. Data generated for tracking simulation.

Data Sets	DATA Features (Sampling Period Δt = 0.03 s)
DATA 1	$x(t) = 50+v_x t$, $y(t) = 50+v_y t$, $t = (1,2,\ldots,100)\Delta t$ v_x = 10 pixel/s, v_y = 20 pixel/s
DATA 2	$x(t) = 50+(1/2)a_x t^2$, $y(t) = 50+(1/2)a_y t^2$, $t = (1,2,,100)\Delta t$ a_x = 5 pixel/s^2, a_y = 15 pixel/s^2
DATA 3	1st Movement: t = (1,2,…,50)t $x(t) = 50+(1/2)a_x t^2$, $y(t) = y(0)+(1/2)a_y t^2$ a_x = 5 pixel/s^2, a_y = 15 pixel/s^2 2nd Movement: t = (51,52,…,100)t $x(t) = x(1.5)+v_x(t-1.5)$, $y(t) = y(1.5)+v_y(t-1.5)$ v_x = 7.5 pixel/s, v_y = 15 pixel/s
DATA 4	$x(t) = 50+30\cos\theta$, $y(t) = 50+30\sin\theta$ 1st Movement: t = (1,2,…,30)t $\theta(t) = (1/2)at^2$, a = π/0.81 rad/s^2 2nd Movement: t = (31,32,…,60)t $\theta(t) = \theta(0.9)+v(t-0.9)$, v = π/0.9 rad/s 3rd Movement: t = (61,32,…,90)t $\theta(t) = \theta(1.8)+\pi/2+(1/2)a(0.9-(t-1.8))^2$, a = $-\pi$/0.81rad/s^2

by Kalman filtering for the cases of <DATA 3> and <DATA 4>.

To test the 3D position measurement, two cameras were assumed, and synthetic points and their image points were generated at distances of 1000, 950, and 900 mm from the stereo cameras. Only radial lens distortion (distortion

Table 2. Tracking results (MSE [pixel^2]).

DATA SET	Method I		Method II (Kalman filter)	
	Prediction	Estimation	Prediction	Estimation
DATA 1	2.11	1.68	1.11	0.83
DATA 2	2.94	2.00	1.65	1.13
DATA 3	2.21	2.02	1.11	0.95
DATA 4	7.90	2.03	14.70	3.03
			8.36*	1.82*

* The diagonal values in the process noise covariance matrix and measurement noise covariance matrix of the Kalman filter were set to 100 and 10, respectively, while both of them were set to 10 for all other cases.

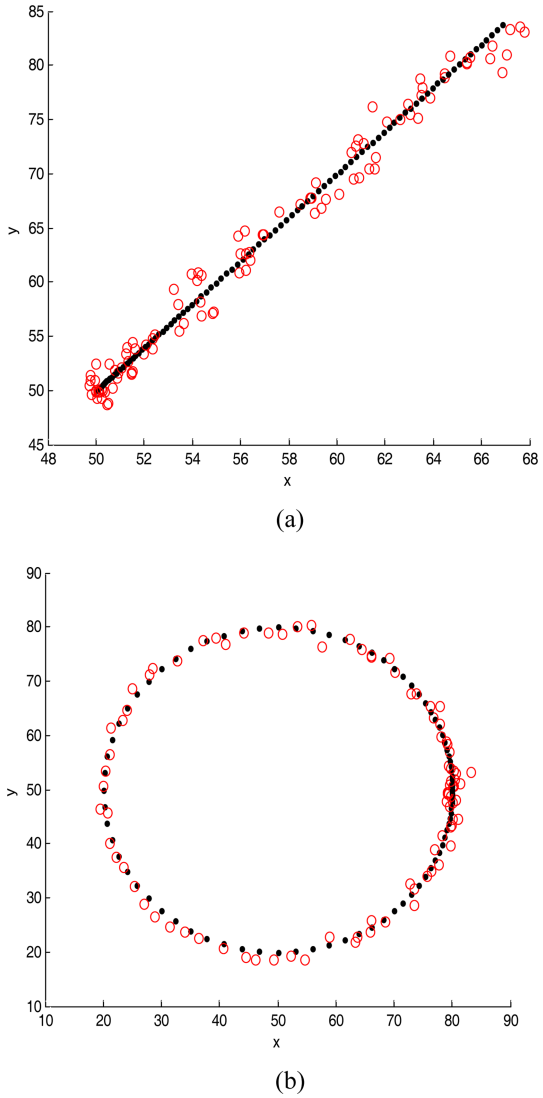

(a) (b)

Fig. 5. Tracking results by Kalman filtering: (a) <DATA 3>, (b) <DATA 4>, where dots are the real positions, while circles are the estimated positions.

parameter k=0.0003) was considered, and additive 1/5 pixel noise in measurement was assumed. When the cameras were

calibrated by the method described in Section 2.3 using points at distances of 900 and 1000 mm, the average accuracy obtained for the test points at 950 mm was 1.52 mm.

4. CONCLUSIONS

We presented vision sensing methods for a robot guided by a laser pointer. A method proposed to detect the laser spot on an image is based on the color, size, and shape of the spot. Even in a cluttered background, our method successfully detected the laser spots on images.

Tracking of the laser spot is required for a robot to understand the command of a user. We tested two spot tracking methods. Although Kalman filtering (Method II) showed better results mostly, the other method (Method I), which used the current spot position to detect the next position, was simple and effective. We conclude that Method II is useful only if the movement model is known. In other cases, particularly if high-accuracy tracking is not an important requirement, Method I can be easily applicable.

Another purpose of laser spot tracking is to increase the detection efficiency. By tracking the laser spot, its position in the next consequent image can be predicted. Then, the spot can be searched only within the ROI around the predicted position. This approach can reduce the processing time and possibility of false detection.

The 3D position of the target point where the laser spot is pointed can be calculated by calibrating two cameras. We tested a method based on the linear pinhole model. The 3D measurement error obtained in our simulation study was approximately 1.5 mm in a distance of approximately 1000 mm.

The methods presented in this paper cover all essential vision sensing procedures when using a laser pointer for robotic guidance. Our study confirmed that the proposed system can be promising for the man–robot interface. However, the system was not mounted into a real robotic hardware system, which is the future work.

ACKNOWLEDGMENT

This research was supported by the Daegu University Research Scholarship Grants.

REFERENCES

[1] H. R. Everett, *Sensors for Mobile Robots: Theory and Application*, A. K. Peters, Ltd. Natick, MA, 1995.

[2] Y. Zhang, H. Wang, and F. Xu, “Object detection and recognition of intelligent service robot based on deep learning”, *Proc. IEEE Conf. Cybern. Intell. Syst. IEEE Conf. Robot. Autom. Mechatron.,* pp. 171-176, 2017.

[3] D. U. Kim, S.-H. Park, and Y. Do, “Vision-based automatic detection of a laser spotlight on a projector screen,” *Proc. Int. Conf. Comput. Commun., Syst.*, 2015.

[4] https://www.technologyreview.com/s/409785/a-robotic-helping-hand/ (retrieved on Jul. 16, 2018).

[5] P. Johansson, “*Robot Cell Calibration Using a Laser Pointer SME Robot”*, M.Sc. Thesis, Lund University, 2007.

[6] J.-H. Kim, J.-C. Lee, and Y.-R. Choi, “LAROB: Laser-guided underwater mobile robot for reactor vessel inspection. *IEEE/ASME Trans. Mechatron*., Vol. 19(4), pp. 1216-1225, 2014.

[7] J. N. Pires, “Robot-by-voice: Experiments on commanding an industrial robot using the human voice”, *Ind. Robot*, Vol. 32(6), pp. 505-511, 2005.

[8] P. Diwan and S. Mitra, "Hand Gesture Controlled Robot", *Artif. Intell. Syst. Mach. Learn.*, Vol. 6(5), pp. 176-179, 2014

[9] https://en.wikipedia.org/wiki/Kalman_filter(retrieved on June. 20, 2018).

[10] Y. Do, “A new linear explicit camera calibration method”, *J. Sensor Sci. & Tech*., Vol. 23(1), pp. 68-73, 2014.